Engineering with Computers (2020) 36:29–42
https://doi.org/10.1007/s00366-018-0686-3

ORIGINAL ARTICLE

Novel approach to predicting blast-induced ground vibration using Gaussian process regression

Clement Kweku Arthur[1] · **Victor Amoako Temeng**[1] · **Yao Yevenyo Ziggah**[2]

Received: 25 August 2018 / Accepted: 14 December 2018 / Published online: 2 January 2019

Abstract
An attempt has been made to propose a novel prediction model based on the Gaussian process regression (GPR) approach. The proposed GPR was used to predict blast-induced ground vibration using 210 blasting events from an open pit mine in Ghana. Out of the 210 blasting data, 130 were used in the model development (training), whereas the remaining 80 were used to independently assess the performance of the GPR model. The formulated GPR model was compared with the other standard predictive techniques such as the generalised regression neural network, radial basis function neural network, back-propagation neural network, and four conventional ground vibration predictors (United State Bureau of Mines model, Langefors and Kihlstrom model, Ambraseys–Hendron model, and Indian Standard model). Comparatively, the statistical results revealed that the proposed GPR approach can predict ground vibration more accurately than the standard techniques presented in this study. The GPR had the highest correlation coefficient (R), variance accounted for, and the lowest values of the statistical error indicators (mean absolute error and root-mean-square error) applied. The superiority of GPR to the other methods is explained by the ability of the GPR to quantitatively model the noise patterns in the blasting data events adequately. The study will serve as a foundation for future research works in the mining industry where artificial intelligence technology is yet to be fully explored.

Keywords Gaussian process regression · Artificial neural network · Ground vibration empirical predictors · Blasting

1 Introduction

The Earth is richly endowed with mineral reserves (raw materials) which are beneficial to the existence of mankind. These raw materials include precious metals such as gold, diamond, silver, bauxite, iron, nickel, manganese, cobalt, platinum, vermiculite, and zirconium. However, these minerals are buried deep down the Earth and, hence, surrounded by a large massive waste rock formation. To have access to these minerals and make it available to mankind, the process of mining is usually employed.

Mining is conventionally done through drill and blast operation through which inclined or vertical holes are drilled into the rock formation. Explosives are then used to fragment the rock mass into smaller pieces, thereby creating shock waves in the drilled holes. The blasting event leads to a high chemical reaction which evolves a huge quantity of energy which starts propagating away in a radial direction. Initially, the intensity of the energy is so high that matter near the walls of the blast holes are crushed and displaced radially. However, as the energy intensity decreases, due to geometric spreading, the energy continues to travel through the in situ rock mass as an elastic ground vibration [1, 2]. The unused energy in fragmenting the in situ rock mass also generates other undesirable effects such as flyrock, noise, air overpressure, and backbreak [3–6]. Moreover, blast-induced ground vibration which is the focus of this study, could cause structural responses and nuisance to humans [7, 8]. In the light of that, it has become a mandatory responsibility of every mining company to monitor the levels of ground vibration during each blast event. This monitoring will provide management of the mine to have the first-hand information

✉ Victor Amoako Temeng
vatemeng@umat.edu.gh

[1] Department of Mining Engineering, Faculty of Mineral Resources Technology, University of Mines and Technology, Tarkwa, Western Region, Ghana

[2] Department of Geomatic Engineering, Faculty of Mineral Resources Technology, University of Mines and Technology, Tarkwa, Western Region, Ghana

on whether the ground vibration levels are below or within the safe levels (standards) set by the Environmental Protection Agency (EPA) of the country.

In general, the vibration monitoring and measurement are done by the use of blasting seismographs. This instrument has a triaxial geophone connected to a processor to collect and analyse the signals. This triaxial geophone contains three mutually perpendicular transducers, each consisting of a spring-loaded moving mass system located within a moving coil to record the three mutually perpendicular components of the motion of the ground particles due to the passage of blasting vibration. These components are: longitudinal (radial) (x), transverse (y), and vertical (z). The particle velocity at a point is the vector sum of the three components at the same instant of time, as shown in Eq. (1) [9]:

$$\text{Particle velocity} = \sqrt{v_x^2 + v_y^2 + v_z^2}, \tag{1}$$

where v_x, v_y, and v_z are the particle velocity in the longitudinal, transverse, and vertical directions, respectively. It is worth mentioning that peak particle velocity (PPV) is the most preferable and frequently used indicator for the evaluation of ground vibration. PPV is the velocity of motion of a particle on or in the ground induced by the passing of the blast vibration waves [9].

Over the years, attempt has been made to relate the contributing factors of ground vibration particle motion to the measured PPV. This led to the development of many empirical models presented in Table 1. As these methods have been applied throughout the scientific literature, Table 1 provides only a summary of the modelling method and a description of terms in the related equations.

The aforementioned empirical models (Table 1) are based solely on two input parameters, namely, distance and maximum charge per delay. Moreover, the empirical predictors are site-specific and, hence, site constants included in the equations (Table 1) must be computed to suit the specific civil or mining industry. Researchers who came up with these models are of the view that the mentioned parameters are the main factors contributing to ground vibration induced by blasting. However, other scholars [2, 19–23 and references therein] argue that the intensity of ground vibration depends on two main groups of parameters, namely controllable and uncontrollable parameters

Table 1 Summary of various PPV empirical predictors

Modelling method	References	Equation	Description
USBM	Duvall and Petkof [10]	$\text{PPV} = k(D/\sqrt{Q})^{-\beta}$	PPV is the peak particle velocity, D is the distance between the blast face to the monitoring station (m), Q is the cooperating charge (kg), and k and β are the site-specific constants to be determined
Langefors–Kihlstrom	Langefors and Kihlstrom [11]	$\text{PPV} = k(Q^{1/2}/D^{3/4})^{\beta}$	
General predictor	Davies et al. [12]	$\text{PPV} = k \cdot D^{-\beta} \cdot Q^{A}$	
Ambraseys–Hendron	Ambraseys and Hendron [13]	$\text{PPV} = k(D/\sqrt[3]{Q})^{-\beta}$	
Indian Standard	Bureau of Indian Standards [14]	$\text{PPV} = k(Q/D^{2/3})^{\beta}$	
Ghosh–Daemen 1	Ghosh and Daemen [15]	$\text{PPV} = k(D/\sqrt{Q})^{-\beta} \cdot \mathrm{e}^{-\alpha \cdot D}$	
Ghosh–Daemen 2	Ghosh and Daemen [15]	$\text{PPV} = k(D/\sqrt[3]{Q})^{-\beta} \cdot \mathrm{e}^{-\alpha \cdot D}$	
Gupta et al.	Gupta et al. [16]	$\text{PPV} = k(D/\sqrt{Q})^{-\beta} \cdot \mathrm{e}^{-\alpha \cdot (D/Q)}$	
CMRI predictor	Roy [17]	$\text{PPV} = n + k(D/\sqrt{Q})^{-1}$	
Rai–Singh	Rai and Singh [18]	$\text{PPV} = k \cdot D^{-\beta} \cdot Q^{A} \cdot \mathrm{e}^{-\alpha \cdot D}$	

Table 2 Factors that affect ground vibration

Controllable parameters		Uncontrollable parameters
Blast design parameters	Explosive parameters	Geotechnical and geomechanical parameters
Hole depth	Explosive type	Rock mass strength
Hole diameter	Maximum charge per delay	Ground water condition
Bench height	Total charge	Discontinuity frequency
Burden	Powder factor	Bedding plane
Spacing	Velocity of detonation (VOD)	
Stemming	Delay time	
sub-drilling	Direction of initiation	
No. of holes and rows		
Hole inclination		

(Table 2) that could be considered and quantified in the development of ground vibration prediction models. The controllable parameters are those that can be changed by the blast engineers, whereas the uncontrollable parameters cannot be changed by the blast engineers [21]. Besides, blast-induced ground vibration is a complex phenomenon with highly nonlinear variable interactions which cannot be adequately modelled using closed-form mathematical equations (Table 1) [24, 25]. In addition, Dindarloo [25] is of the view that lack of generalisability is a common phenomenon inherent in the empirical prediction models (Table 1) because of the number of input parameters considered.

To address these issues, several research works have attempted to explore soft-computing technology as alternative technique that can accommodate more contributing factors, adequately model nonlinear systems, and produce accurate results. Until now, the notable methods found in the literature for predicting blast-induced ground vibration include artificial neural network (ANN), support vector machines (SVM), fuzzy logic, neuro-fuzzy inference systems (ANFIS), classification and regression tree (CART), hybrid intelligent methods, group method of data handling (GMDH), and genetic expression [25–36]. These techniques have been found to outperform the empirical predictors due to their ability to learn, adapt, and generalise well to the data set introduced to them without a priori knowledge of the mathematical association between input and output parameters. Thus, they have the ability to model correctly the complex nonlinear and dynamic system interactions of the blast design, explosive, and geotechnical and geomechanical parameters. The soft-computing techniques also have the capability to tolerate imprecision, uncertainty, approximate reasoning, and partial truth to achieve tractability and robustness on simulating human thinking to match up with reality [37].

It is noteworthy that the literature is replete with the application of ANN and is regarded as the most standard and prominently used soft-computing technique for the prediction of ground vibration. Some important studies are in Refs. [19, 24, 38–50]. In spite of its wide applicability, ANN suffers from many practical limitations such as slow convergence speed, poor generalisation performance, overfitting problems, and no reasoning capability. It also requires a lot of manual tuning of the model parameters to achieve global optimum. There is also local minima sticking with suboptimal solutions [51–53]. Furthermore, there is no proper method to determine the number of hidden neurons other than the sequential trial and error process [54, 55]. It is agreeable that a model should be simple and easily applicable to solving real-world problem. Therefore, to address and overcome some of the weaknesses of the ANN as aforementioned to give better blast-induced ground vibration prediction results and improve convergence, there is the need to explore the other alternative soft-computing methods.

In that respect, this study adopts Gaussian process regression (GPR) for modelling and prediction of blast-induced ground vibration. GPR is a type of Bayesian non-parametric method which can handle the uncertainties in data in a principled manner. It has the possibility to include various kinds of prior knowledge into the model. The number of model parameters, which need to be optimised in the GPR, is less than that of the ANN. Moreover, the tuning of these parameters is carried out using optimiser unlike the ANN which requires human interferences. In addition, the existence of noise in the measured data can be modelled quantitatively in the GPR, thereby having a little impact on the prediction accuracy of the developed GPR model [56]. GPR has been successfully and widely adopted for solving diverse engineering and science related problems [54, 57–61 and references therein]. Although the GPR technique is already in use, quality evaluation of the method in the area of blast-induced ground vibration prediction studies has not been exploited. Furthermore, the GPR technique has not been compared with the benchmark ANN methods to ascertain its reliability in ground vibration prediction. Therefore, taking cognisant of the earlier enumerated mathematical conveniences and benefits provided by the GPR, the paper aims to:

(i) investigate the viability of GPR as a novel approach for predicting blast-induced ground vibration using blast event data from an open pit mine in Ghana;
(ii) make a comparative study between the developed GPR model and benchmark methods of back-propagation neural network (BPNN), radial basis function neural network (RBFNN), generalised regression neural network (GRNN), and four empirical ground vibration predictors, namely, United State Bureau of Mine (USBM) model, Indian Standard model, Ambraseys–Hendron model, and Langefors and Kihlstrom model.

The rest of the paper is organised as follows. Section 2 presents a brief description of the study area. Section 3 provides a concise overview on the theoretical concept of the proposed GPR approach. Section 4 elaborates on the data set used, post processing, and how the GPR model was developed. In Sect. 5, a description of the statistical evaluators used to ascertain the predictive capabilities of the various models utilised is presented. In Sect. 6, the best GPR model is selected. Prediction results from the selected GPR model are compared with the results produced by BPNN, RBFNN, GRNN, and conventional empirical techniques (USBM model, Langefors and Kihlstrom model, Ambraseys–Hendron model, and Indian Standard model). Section 7 ends the study with conclusions.

2 Brief description of study area

This study was carried out in an open pit mine in Tarkwa, Ghana. The Mine is bounded between latitude 5°16′ North and longitude 1°59′ West in the south-western corner of Ghana. With respect to the map of Ghana, the Mine is situated 89 km northwest from the port of Takoradi and 6.5 km south of Tarkwa [62]. Figure 1 shows the study area.

The open pit mine (study area) has three pits, namely: pit M, pit N, and pit O. Active mining is currently ongoing in pit O. This pit has been subdivided into O South West (OSW), O South East (OSE), O Central West (OCW), O Central East (OCE), and O North (ON). The Mine employs drill and blast techniques to fragment in situ rock formation into suitable rock sizes which are hauled using Volvo AD35, Komatsu HD 465, and CAT 777F rear dump trucks to either the run-of-mine (ROM) or waste dump. Blasting is done with Emulsion EX 7000, 250 g Pentolite booster, a 500 ms down the hole, and either a 25 ms or 42 ms DDX NONEL detonator supplied by Maxam International. The bulk explosives used for the column charge are the Emulsion EX 7000. A 3 m stemming height is applied at the study area with stemming material (gravels) of 15 mm blended with 20 mm to ensure effective confinement. The surface connectors used for the trunk line connections include 17 ms, 42 ms, and 67 ms with an NONEL MS firing method. Three main types of rock formation characterise the study area. These rock types are greenstones, turbidites (metatuffs), and manganiferous horizon. The manganiferous horizon makes up the ore deposit, while the greenstones and metatuffs form the host rocks. The ore mined are the detrital ore, oxide ore, carbonate-oxide ore (carbox), and the manganese carbonate ore. The existence of these different types of ore is due to the different rate of alteration and weathering at the time of formation [62]. The manganese carbonate ore is processed by crushing to aggregates of 100 mm, 40 mm, and 20 mm, which are designated as lumps, logs, and fines, respectively. The crushing plant has a capacity of 300 metric tons per hour. The finished product from the plant is stockpiled and further conveyed to the port in Takoradi, Ghana for export [63]. Monitoring of blast-induced ground vibration is carried out by the environmental department of the Mine. Their monitoring station is located on flat ground near the first house to the mine pit of the nearest community. The monitoring is done using a 3000 EZ Plus Portable seismograph.

3 Methodology

In this section, a concise theoretical concept on the proposed Gaussian process regression will solely be presented. Theories on the benchmark artificial neural network techniques (BPNN, RBFNN, and GRNN), and empirical techniques (USBM model, Langefors and Kihlstrom model, Ambraseys–Hendron model, and Indian Standard model) which have been widely and successfully applied in blast-induced ground vibration prediction will not be treated here. A detailed information on them can be found in [10, 11, 13, 14, 64–67].

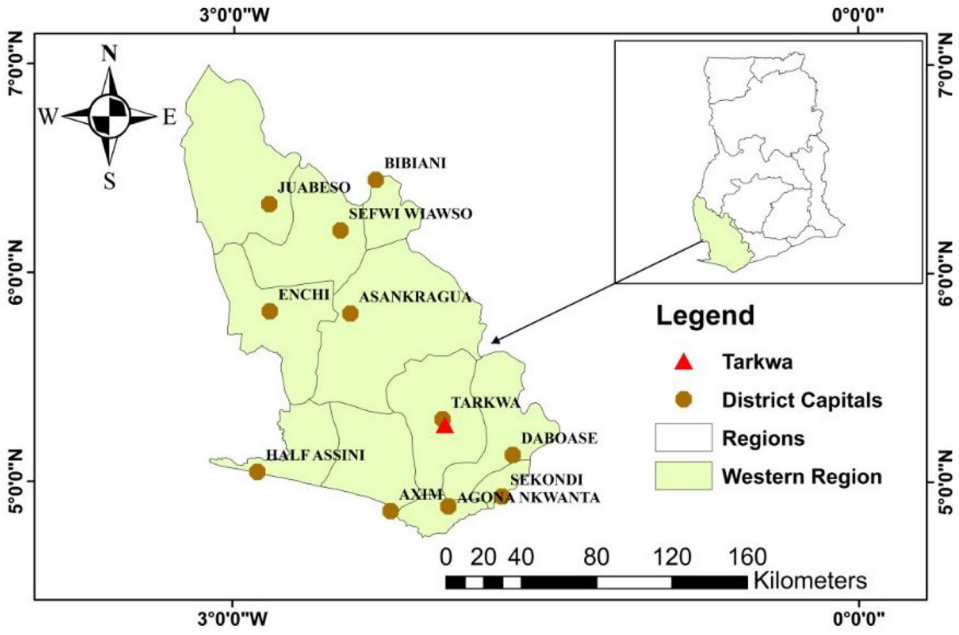

Fig. 1 Study area

3.1 Gaussian process

A Gaussian process is a stochastic process (a collection of random variables), such that every finite collection of the random variables has a joint Gaussian distribution [68]. A Gaussian process $t(x)$ is parameterised by a mean function $m(x)$ and a covariance function (or kernel) $k(x, x')$ evaluated at points x and x'. These functions are defined in Eqs. (2) and (3) as follows:

$$m(x) = E(t(x)) \tag{2}$$

$$\mathrm{Cov}(t(x), t(x')) = k(x, x';\theta) = E((t(x) - m(x))(t(x') - m(x'))), \tag{3}$$

where θ denotes the set of hyperparameters. A Gaussian process $t(x)$ is, hence, expressed in Eq. (4) as follows:

$$t(x) \sim \mathrm{GP}(m(x), k(x, x')), \tag{4}$$

where GP stands for gaussian process. This means that the function $t(x)$ is distributed as a Gaussian process with mean $m(x)$ and covariance function $k(x, x')$.

3.1.1 Gaussian process for regression

The goal of every regression problem is to model the dependence of a response variable y on some predictor variables, x_i. Each response variable y can be related to an underlying arbitrary regression function $t(x)$ with an additive independent identically distributed Gaussian noise (ε) which represents the noise component from the data. This is expressed in the following equation:

$$y = t(x) + \varepsilon. \tag{5}$$

The noise ε has zero mean and variance σ_n^2 that is $\varepsilon \sim N(0,\sigma_n^2)$. The Gaussian process represented in Eq. (4) becomes Eq. (6) [69]:

$$t(x) \sim \mathrm{GP}(m(x), k(x, x') + \sigma_n^2 I), \tag{6}$$

where I is the identity matrix. Based on the additive nature of the noise ε and the marginalization property of GPs, the joint distribution of the training output y at locations X and test outputs f_* at test points X_* is given in Eq. (7) [69]:

$$\begin{bmatrix} y \\ f_* \end{bmatrix} \sim N\left(\begin{bmatrix} m(X) \\ m(X_*) \end{bmatrix}, \begin{bmatrix} k(X, X + \sigma_n^2 I) & k(X, X_*) \\ k(X_*, X) & k(X_*, X_*) \end{bmatrix} \right). \tag{7}$$

Conditioning the joint Gaussian prior distribution based on X, y, and X_*, the predictive distribution is given in the following equation:

$$p\left(y_* \middle| X, y, X_*\right) \sim N\left(\bar{y}_*, \mathrm{var}\left(y_*\right)\right), \tag{8}$$

where $\bar{y}_*$ (Eq. 9) is the predictive mean and $\mathrm{var}(y_*)$ (Eq. 10) is the predictive variance [69]:

$$\bar{y}_* = m(X_*) + k(X_*, X)[k(X, X) + \sigma_n^2 I]^{-1}(y - m(X)) \tag{9}$$

$$\mathrm{var}(y_*) = k(X_*, X_*)[k(X, X) + \sigma_n^2 I]^{-1} k(X, X_*). \tag{10}$$

3.1.2 Covariance function

A covariance function is the central component in a Gaussian process regression model [68]. Therefore, selecting the appropriate covariance function is crucial to the determination of the sample function being modelled. Given that the input points which are closely related are likely to have similar target values; likewise, test point near a training point should have a corresponding target value close to the training point. With this analogy, a test point's target value can be predicted. This measure of similarity is expressed by the covariance function [70]. There are a number of common covariance functions available in the literature. Some of these include: constant covariance function, linear covariance function, Gaussian noise covariance function, Ornstein–Uhlenbeck covariance function, squared exponential covariance function, Gamma exponential covariance function, Matérn Class of covariance function, Periodic covariance function, Rational quadratic covariance function, and others [68]. However, it is notable in the literature that the squared exponential is the commonly used covariance function [71].

3.1.3 Training a Gaussian process regression model

The parameters of the mean function and covariance (kernel) functions are called the hyperparameters of the Gaussian process [70]. These hyperparameters define the behaviour of the GPR model. To train and formulate a GPR model, all the hyperparameters associated with the mean and covariance function must be learned. This can be done through either optimisation or sampling techniques. However, the widely used approach is to maximise the log marginal likelihood (Eq. 11) [55]:

$$\log p(y|X, \theta) = -\frac{1}{2} y^{\mathrm{T}} \left(K + \sigma_n^2 I\right)^{-1} y - \frac{1}{2} \log \left|K + \sigma_n^2 I\right| - \frac{n}{2} \log 2\pi, \tag{11}$$

where y^{T} is the transpose of vector y and θ is a vector containing all the hyperparameters.

To maximise the log marginal likelihood, the conjugate gradient method is an efficient gradient-based optimisation algorithm that can be used [72].

4 Model development

In this section, information on the data used, model formulation procedure, and the proposed GPR model developed have been presented.

4.1 Data acquisition and processing

A total of 210 historic blast data set acquired from the Mining and Environmental Department of an Open Pit Mine in Tarkwa, Ghana were used in this study. The data set involved the following parameters: number of blast holes; cooperating charge (kg); distance between blasting point and monitoring station (m); hole depth (m); powder factor (kg/m^3); burden (m); spacing (m); peak particle velocity (PPV) (mm/s). For the development of the GPR model and the other investigated methods (BPNN, RBFNN, and GRNN), 6 out of the 8 parameters were used. The input parameters used include the number of blast holes, cooperating charge (kg), distance between blasting point and monitoring station (m), hole depth (m), and powder factor (kg/m^3). The output parameter is the PPV (mm/s). The burden and spacing parameters were not considered due to their constant values used by the Mine for each blast. It is worth noting that these parameters were carefully measured. Table 3 outlines the statistical range of measured parameters used in this research. The values for the number of blast holes, cooperating charge (kg), hole depth (m), and powder factor, were computed and obtained from the blasting designs. Global positioning system (GPS) measurements were used to determine the distance between blasting point and monitoring station. Here, the GPS-recorded coordinates between the blasting face and that of the monitoring station were used to calculate the distance. The values of PPV were measured by a 3000 EZ Plus Portable seismograph. It should be noted that the monitoring of the ground vibration was done at the nearest community to the mining pit. Correlation coefficient matrix, which outlines the strength of the relationship between the input parameters [number of blast holes, distance between blasting point and monitoring station, cooperating charge (kg), hole depth (m), and powder factor], and measured PPV is presented in Table 4.

To generate good predictions, ANN requires enough data for training. However, if the training data are more than enough, it will cause overfitting, whereby the model cannot perform well with unseen data. Despite the fact that there is no universally accepted ratio for splitting the data, the hold-out cross-validation technique which has been widely and successfully used in ANN modelling was adopted in the present for the data partitioning. Therefore, based on the principle of hold-out cross-validation, it is important that the training data set must be more than the testing set. Here, the entire 210 data set was partitioned into two subsets: training and testing sets. In that regard, the first partition which formed the training data set is made up of 130 data points representing 62% of the entire blasting data. The second partition which formed the testing data set involved the remaining 38% of the data representing 80 points. The training data were purposely selected to represent the entire characteristic of the whole data in the study area. Likewise, the testing data chosen are evenly distributed across the area of study. Here, the training data set was used to build and train the GPR model and the other methods investigated in this study, while the testing data set was used to judge how the model will perform with unseen data.

In the model construction, the training and testing data sets were normalised as part of the pre-processing step. The essence is to ensure constant variability and reduce the impact

Table 3 Statistical description of the data set

Parameters	Unit	Minimum	Maximum	Average	Standard deviation
Number of blast holes	–	19	355	122.50	52.37
Explosive per blast hole	kg	11.60	123.49	90.08	19.54
Distance from blasting point	m	573	1500	915.01	234.62
Hole depth	m	3.73	12.58	10.45	1.14
Powder factor	kg/m^3	0.10	0.97	0.69	0.15
Peak particle velocity	mm/s	0.13	1.65	0.79	0.32

Table 4 Correlation coefficient matrix between input parameters and measured PPV

	Number of blast holes	Cooperating charge (kg)	Distance from blasting point (m)	Hole depth (m)	Powder factor (kg/m^3)	PPV (mm/s)
Number of blast holes	1					
Cooperating charge (kg)	0.0585	1				
Distance from blasting point (m)	−0.1161	−0.1862	1			
Hole depth (m)	−0.0528	0.5527	−0.1431	1		
Powder factor (kg/m^3)	0.1206	0.7954	−0.1639	0.2460	1	
PPV (mm/s)	0.4715	0.4700	−0.6957	0.2985	0.5153	1

of variables with high variance to have minimal effects in the model prediction outcomes. This is because the data sets have different range of values with different physical units; Eq. (12) [73] was used to normalise the data into the range [−1, 1]:

$$M_i = M_{\min} + \frac{(M_{\max} - M_{\min}) \times (N_i - N_{\min})}{N_{\max} - N_{\min}}, \tag{12}$$

where M_i is the normalised data, N_i represents the measured blast data, and $N_{\max}$ and $N_{\min}$ represent the maximum and minimum values of the measured blast data with $M_{\min}$ and $M_{\max}$ values set at −1 and 1, respectively.

4.2 Proposed GPR model

In this study, a simple mean function with constant, c, was used. For selecting the optimum covariance function for the proposed GPR model, the following covariance functions as expressed in Eqs. (13)–(17) [68] were tried and tested.

i. Squared exponential covariance function:

$$k(x_i, x_j) = \sigma_{\mathrm{f}}^2 \exp\left[\frac{-d^2}{2\ell^2}\right]. \tag{13}$$

ii. Exponential covariance function:

$$k(x_i, x_j) = \sigma_{\mathrm{f}}^2 \exp\left[-\frac{d}{\ell}\right]. \tag{14}$$

iii. Rational quadratic covariance function:

$$k(x_i, x_j) = \sigma_{\mathrm{f}}^2 \exp\left[1 + \frac{d^2}{2\alpha\ell^2}\right]^{-\alpha}. \tag{15}$$

iv. Matérn 3/2 covariance function:

$$k(x_i, x_j) = \sigma_{\mathrm{f}}^2 \left(1 + \frac{\sqrt{3}d}{\ell}\right) \exp\left(-\frac{\sqrt{3}d}{\ell}\right). \tag{16}$$

v. Matérn 5/2 covariance function:

$$k(x_i, x_j) = \sigma_{\mathrm{f}}^2 \left(1 + \frac{\sqrt{5}d}{\ell} + \frac{5d^2}{3\ell^2}\right) \exp\left(-\frac{\sqrt{5}d}{\ell}\right), \tag{17}$$

where $d = \left\| x_i - x_j \right\|$ is the Euclidean distance between point x_i and x_j, σ_{f}^2 is the signal variance of function, α is the shape parameter for the rational quadratic covariance, and ℓ is the length scale. Due to the mean function, covariance function, and the noisy observations in data, the hyperparameters θ that were optimised in this study include: constant (c), σ_{f}^2, ℓ, α, and σ_{n}^2. σ_{n}^2 is the noise variance.

5 Evaluation of model performance

To evaluate the prediction performance of the proposed GPR model to the BPNN, RBFNN, GRNN, USBM model, Langefors and Kihlstrom model, Ambraseys–Hendron model, and Indian Standard model, five statistical indicators namely: mean square error (MSE), root-mean-square error (RMSE), mean absolute error (MAE), correlation coefficient (R), and variance accounted for (VAF). They are mathematically expressed in Eqs. (18)–(23) [6, 74–79]:

$$\mathrm{MSE} = \frac{\sum_{i=1}^{N} (O_i - P_i)^2}{N} \tag{18}$$

$$\mathrm{RMSE} = \sqrt{\mathrm{MSE}} = \sqrt{\frac{\sum_{i=1}^{N} (O_i - P_i)^2}{N}} \tag{19}$$

$$\mathrm{MAE} = \frac{\sum_{i=1}^{N} |O_i - P_i|}{N} \tag{20}$$

$$R = \frac{\sum_{i=1}^{N} (O_i - \bar{O})(P_i - \bar{P})}{\sqrt{\sum_{i=1}^{N} (O_i - \bar{O})^2} \times \sqrt{\sum_{i=1}^{N} (P_i - \bar{P})^2}} \tag{21}$$

$$VAF = \left[1 - \frac{\mathrm{var}(O_i - P_i)}{\mathrm{var}(O_i)}\right] \times 100, \tag{22}$$

where N is the total number of samples, O_i are the observed values, P_i are the predicted values, $\bar{O}$ is the mean of the observed values, and $\bar{P}$ is the mean of the predicted values.

Graphical comparison of the efficiency of the various models in predicting ground vibration was carried out. This was done by plotting the observed PPV against predicted PPV with a 1:1 line, a 95% confidence interval (CI) (Eqs. 23), and 95% prediction interval (PI) (Eq. 24):

$$\mathrm{CI} = \bar{P} \pm Z_{\alpha/2} \frac{\sigma}{\sqrt{n}}, \tag{23}$$

where $\bar{P}$ is the mean of the predicted values, σ is the population standard deviation, $Z_{\alpha/2}$ is the Z value for the desired confidence level α, and n is the number of predicted values. At a 95% confidence interval, $Z_{\alpha/2} = 1.96$:

$$\mathrm{PI} = P_i \pm t_{(\alpha/2, n-2)} \mathrm{SD} \sqrt{1 + \frac{1}{n} + \frac{(O_i - \bar{O})^2}{\sum (O_i - \bar{O})^2}}, \tag{24}$$

where n is the total number of samples, O_i are the observed PPV values, P_i are the predicted PPV values, $\bar{O}$ is the mean

of the observed PPV values, $t_{(\alpha/2,n-2)}$ is the α-level quantile of a t-distribution with n − 2 degrees of freedom, and SD is the standard deviation of the residuals (Eq. 25):

$$s = \sqrt{\frac{\sum (O_i - P_i)^2}{n-2}}. \tag{25}$$

6 Results and analysis

In this section, the results of the various techniques considered are presented. In Sect. 6.1, discussion on the GPR models formed based on the different covariance functions used are presented. In Sect. 6.2, a detailed comparison of the proposed GPR model with the other benchmark techniques are presented.

6.1 GPR model results

Using the MSE and R criteria, the comparative results obtained by the various GPR models using the testing data sets are presented in Table 5.

From Table 5, it can be observed that the various GPR models had very close R values in the range 0.8300–0.8339 and MSE values falling in the range 0.0245–0.0252. These results confirm that the various GPR models can accurately predict blast-induced ground vibration levels. This is because they all gave R values close to 1 and MSE values very close to 0, indicating good predictive capability. The results further indicated that the covariance functions (Table 5) utilised have similar predictive capabilities. However, in comparison, the GPR model with the Matérn 3/2 covariance function had the highest R value and the second least MSE to the exponential covariance function. The Matérn 3/2 was then selected as the optimum because from Table 5, it is noticeable that the MSE difference between the Matérn 3/2 and exponential covariance function is 0.0001, thus, having very negligible influence on the GPR model outcome. By virtue of the results (Table 5), the selected proposed GPR model valid for blast-induced ground vibration prediction has a constant mean function and Matérn 3/2 covariance function.

Table 5 Test results of the various Gaussian process regression model

Model	Covariance type	R	MSE
GPR	Squared exponential	0.8300	0.0252
GPR	Exponential	0.8325	0.0245
GPR	Matérn 3/2	0.8339	0.0246
GPR	Matérn 5/2	0.8328	0.0248
GPR	Rational quadratic	0.8317	0.0250

6.2 Comparison of GPR model and other investigated techniques

The same data sets (training and testing) applied to the GPR technique were further used to develop models based on the BPNN, RBFNN, GRNN, and empirical predictors (USBM model, Langefors and Kihlstrom model, Ambraseys–Hendron model, and Indian Standard model). The BPNN developed consists of three layers: input, hidden, and output layers. One hidden layer was used in this study, because it has been proven in the literature to have the capability to universally approximate any complex problem [80]. Due to the nonlinearity of the input data to the network, the hyperbolic tangent sigmoid and linear transfer functions were utilised in the hidden and output layers. Training of the BPNN was done using the Levenberg–Marquardt algorithm [81]. The optimum BPNN obtained for this study had five inputs, one neuron in the hidden layer and one output, with the structure [5-1-1]. The developed RBFNN also had three layers namely: input, hidden, and output layer. The Gaussian radial basis function was used in the hidden layer to process the input data to the network. Training was done using the gradient descent algorithm [82]. In the RBFNN, the width parameter of the Gaussian radial basis function and the maximum number of neurons in the hidden layer are the only parameters that need to be adjusted during the training phase. After training, width parameter and maximum number of neurons of 1.6 and 13 which had the lowest MSE and highest R were selected. This led to an optimum RBFNN model having 5 inputs, 13 hidden neurons, and 1 output with structure [5-13-1]. The developed GRNN has four layers: input, pattern, summation, and output layers. The training parameter adjusted to develop the GRNN is the width parameter. In this study, the selected width parameter that gave better MSE and R results was 0.53. With regards to the development of the empirical predictors, site constants were determined. These constants were obtained using regression analysis. Table 6 presents the respective determined model equations for the empirical techniques utilised in this study. The empirical equations utilised in this study have served as benchmark methods over the years when comparison are made with soft-computing methods [38, 44, 83–86 and references there in]. Hence, the present authors saw it as an opportunity to apply and compare them to the proposed GPR technique.

Table 6 Formulated models of the empirical techniques

Empirical technique	Equations
USBM	$\mathrm{PPV} = 300.7[D/(Q)^{1/2}]^{-1.319}$
Indian Standard	$\mathrm{PPV} = 0.7676[Q/D^{2/3}]^{0.938}$
Ambraseys–Hendron	$\mathrm{PPV} = 1724.4[D/(Q)^{1/3}]^{-1.464}$
Langefors and Kihlstrom	$\mathrm{PPV} = 61.406[Q^{1/2}/D^{3/4}]^{1.5475}$

Table 7 Developed models' performance for predicting PPV

Method	Performance criteria			
	RMSE	MAE	*R*	VAR (%)
GPR-Matérn 3/2	0.1568	0.1302	0.8338	68.87
BPNN	0.1873	0.1543	0.8294	66.31
GRNN	0.1760	0.1503	0.8288	66.40
RBFNN	0.1829	0.1471	0.8223	65.34
USBM	0.2369	0.1818	0.7622	39.32
Ambraseys–Hendron	0.2566	0.2009	0.7466	28.02
Indian Standard	0.1849	0.1504	0.7554	56.97
Langefors–Kihlstrom	0.2136	0.1630	0.7833	49.43

In addition, the empirical predictors applied in this study (Table 6) are being used in the Ghanaian mining industry (study area) for blast-induced ground vibration prediction.

A summary of the statistical comparison of the developed GPR and other investigated methods is presented in Table 7.

From Table 7 it can be observed that the GPR-Matérn 3/2 model had the lowest RMSE and MAE of 0.1568 mm/s and 0.1302 mm/s, respectively. These statistical results indicate that the developed GPR-Matérn 3/2 model PPV predictions marginally deviated from the observed PPV. The reason being that the closer the statistical error indicator (MAE and RMSE) is to zero, the better the model could approximate closely the observed data. Comparatively, it can be observed that the soft-computing methods (GPR-Matérn 3/2 model, BPNN, GRNN, and RBFNN) showed a greater strength of relationship and linear dependence between their predicted and observed PPVs than the empirical methods. This is evident in Table 7 where the GPR-Matérn 3/2 model, BPNN, GRNN, and RBFNN had *R* values above 0.8 while the empirical techniques had below 0.8. This indicates that the predicted PPV values from the soft-computing methods correlate well with the observed PPV than the other models presented in this study. In comparison, the GPR-Matérn 3/2 model was superior to all the methods by exhibiting the highest *R* value of 0.8338. In Table 7, it can also be observed that, the GPR-Matérn 3/2 approach gave the highest VAF value followed by the other ANN techniques and empirical predictors. In this study, the VAF was used to verify the correctness of the models and how well they could approximate the unseen data set [87]. That is, a model with a VAF value closest to 100% is the most accurate among candidate models. It can, thus, be inferred from Table 7 that the GPR-Matérn 3/2 with the highest VAF value of 68.87% could produce more promising and satisfactory results than the other methods tested. The strength of the GPR-Matérn 3/2 could be attributed to its intrinsic ability to add prior knowledge and specifications about the shape of the model by learning the hyperparameters which are relational to the training and testing data. This helps to capture the uncertainties in the data using the noise variance hyperparameter in the model formulation stage.

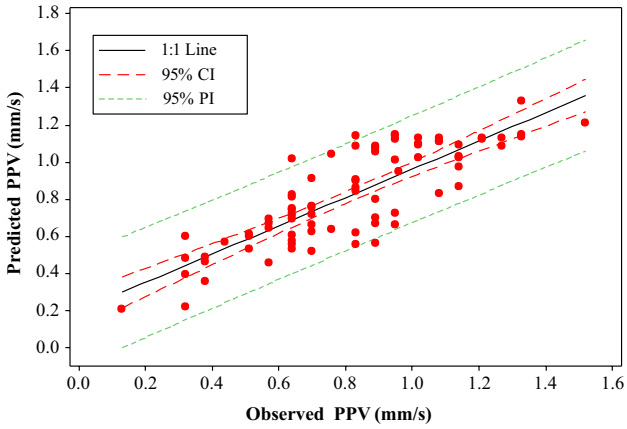

Fig. 2 Observed PPV versus predicted PPV by GPR-Matérn 3/2

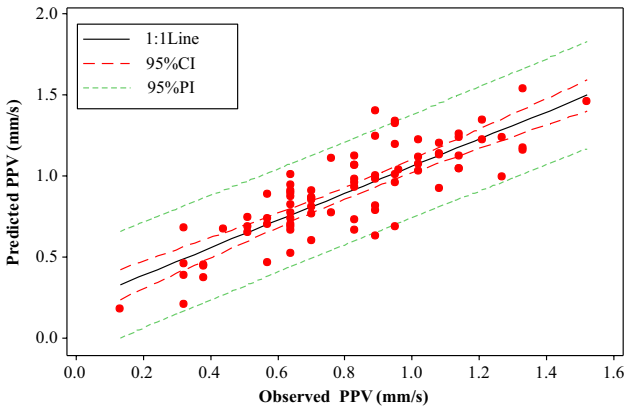

Fig. 3 Observed PPV versus predicted PPV by BPNN

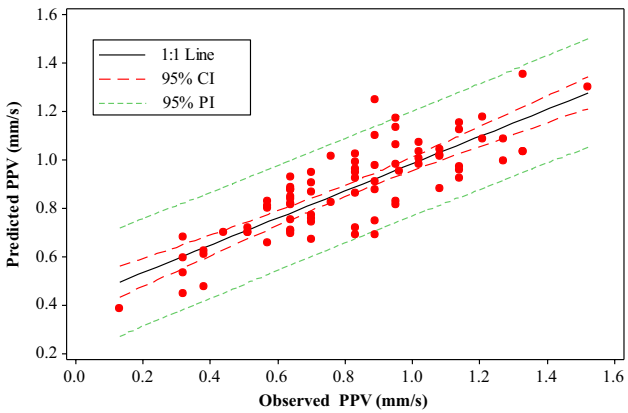

Fig. 4 Observed PPV versus predicted PPV by GRNN

Scatter plots along with the regression line, 95% PI, and CI for the various models are presented in Figs. 2, 3, 4, 5,

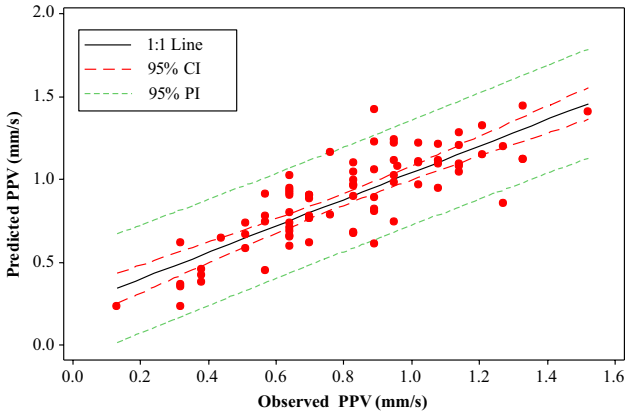

Fig. 5 Observed PPV versus predicted PPV by RBFNN

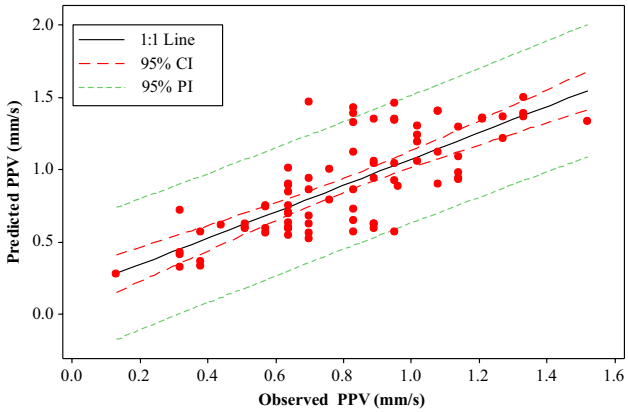

Fig. 6 Observed PPV versus predicted PPV by USBM

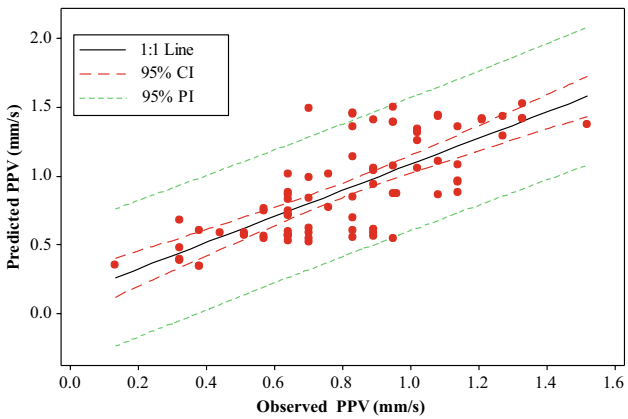

Fig. 7 Observed PPV versus predicted PPV by Ambraseys–Hendron

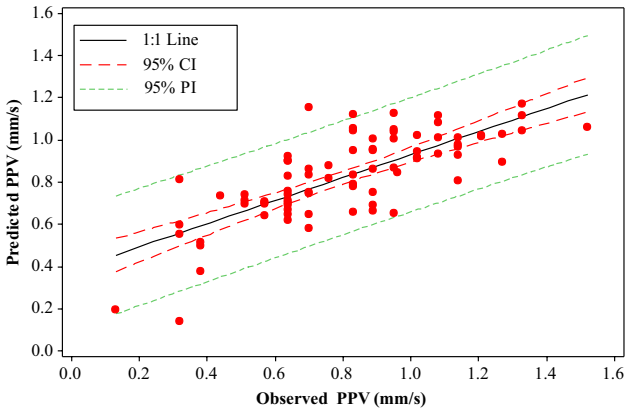

Fig. 8 Observed PPV versus predicted PPV by Indian Standard

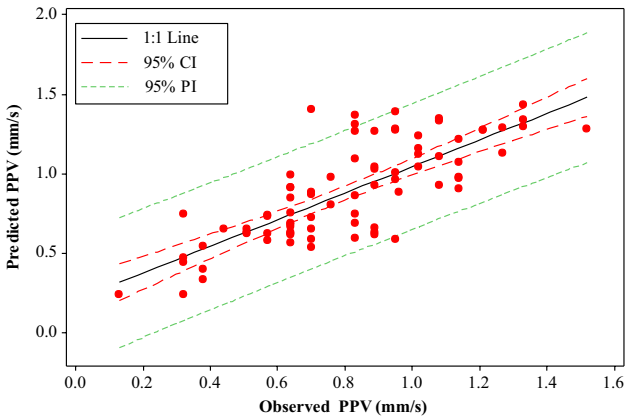

Fig. 9 Observed PPV versus predicted PPV by Langefors–Kihlstrom

6, 7, 8, and 9. A critical look at Fig. 2, 3, 4, 5, 6, 7, 8, and 9 shows that the 1:1 line for each model fell in between the 95% CI lines. This means that there is a 95% probability that the true best-fit line for the population data lies within the CI. It can also be observed that 96% of the predicted PPV values fell within the 95% PI lines. This indicates that, when these models are used to predict new PPV values, there is a 95% probability that 96% of the predicted PPV values will fall into the prediction interval. Overall, visual inspection of the various scatter plots revealed that the predictions produced by GPR-Matérn 3/2, BPNN, GRNN, and RBFN had a narrower prediction interval bandwidth than USBM, Ambraseys–Hendron, Langefors–Kihlstrom, and Indian standard model. The comparative results showed that the proposed GPR-Matérn 3/2 model is superior to the benchmark techniques and a promising tool for modelling and predicting blast-induced ground vibration. A comparison of the predicted and measured PPV using only the testing data sets is illustrated as an additional information in Fig. 10. The results demonstrate that predictions through GPR model are more acceptable in comparison with BPNN, GRNN, RBFNN, and empirical models. Furthermore, due to the environmental impacts of blasting operations which leads to severe damage to nearby residence and structure, accurate prediction of ground vibration intensity is key in controlling and minimising its occurrence. For this reason,

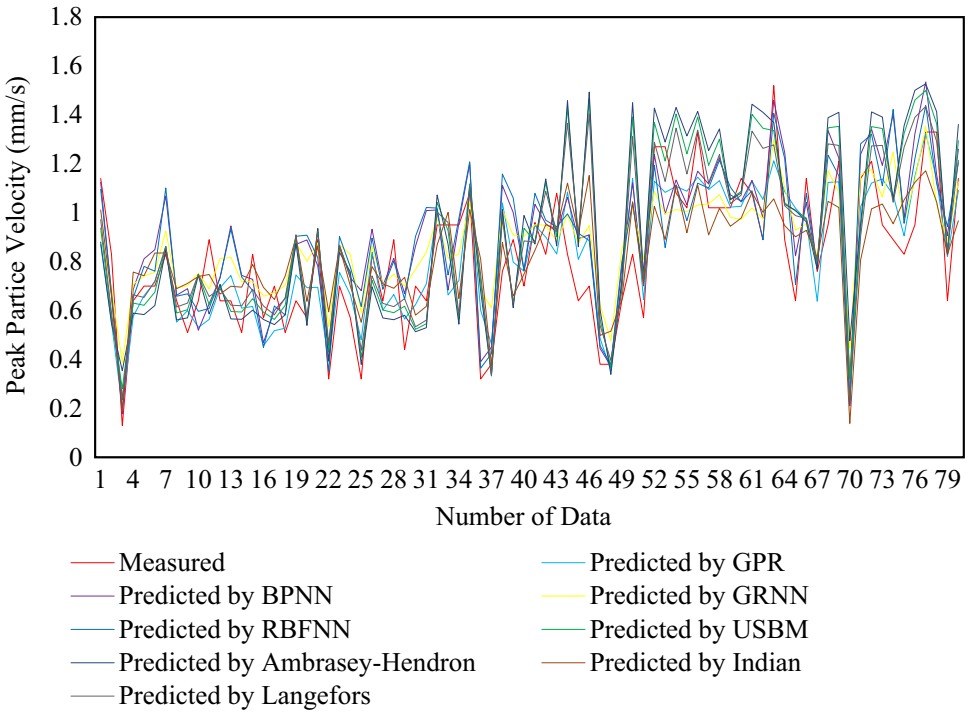

Fig. 10 A comparison of the predicted PPV values by predictive models and the measured PPV

any predictive model that produces more accurate prediction is of utmost importance to the blast engineer. Therefore, looking at the statistical results related to the proposed GPR and the other methods, this study reveals the GPR as being more accurate and as such should be adopted by the blast engineer in predicting blast-induced ground vibration.

7 Concluding remarks

In this study, a novel approach to predict ground vibration using the Gaussian process regression (GPR) has successfully been applied. Five different GPR models were developed based on different types of covariance functions using blast data from an Open Pit Mine in Ghana. The GPR models developed and analysed were the squared exponential, exponential, Matérn 3/2, Matérn 5/2, and rational quadratic. Based on the highest correlation coefficient and lowest mean square error criteria, the Matérn 3/2 was the selected covariance of the proposed GPR model. The proposed GPR-Matérn 3/2 model was successfully compared with the other predictive benchmark techniques of BPNN, RBFNN, GRNN, and four empirical techniques (USBM model, Langefors and Kihlstrom model, Ambraseys–Hendron model, and Indian Standard model). The results showed that the GPR-Matérn 3/2 model yields predicted PPV that is better and consistent with the observed PPV than the other methods considered. The GPR-Matérn 3/2 gave the lowest RMSE and MAE of 0.1568 mm/s and 0.1302 mm/s respectively. It also had the highest correlation coefficient of 0.8339, and accounted for the highest percentage of the variability between the measured and predicted PPV with a VAR value of 68.87%. On the basis of the results obtained, it was concluded that the proposed GPR-Matérn 3/2 model has shown promising application potential in blast-induced ground vibration prediction and can serve as suitable substitute to the other benchmark techniques presented in this study. The efficiency of the proposed GPR-Matérn 3/2 approach was attributed to its intrinsic ability to add prior knowledge and specifications about the shape of the model by learning the hyperparameters. However, the underlining limitation of this study is the lack of application of a specific covariance function. That is, one has to iteratively determine the best covariance that will best generalise the data set. This is because the performance of GPR models is highly dependent on the covariance function (or kernel) used. This makes it cumbersome and time consuming. For future studies, automating the selection of the covariance function by combining with metaheuristic algorithm to improve the GPR prediction ability could be explored.

Acknowledgements The authors would like to thank the Ghana National Petroleum Corporation (GNPC) for providing funding to support this work through the GNPC Professorial Chair in Mining Engineering at the University of Mines and Technology (UMaT), Ghana.

References

1. Gokhale BV (2011) Rotary drilling and blasting in large surface mines. CRC Press/Balkema, Leiden

2. Hasanipanah M, Monjezi M, Shahnazar A, Armaghani DJ, Farazmand A (2015) Feasibility of indirect determination of blast induced ground vibration based on support vector machine. Measurement 75:289–297
3. Monjezi M, Rezaei M, Yazdian A (2010) Prediction of backbreak in open-pit blasting using fuzzy set theory. Expert Syst Appl 37(3):2637–2643
4. Hasanipanah M, Faradonbeh RS, Armaghani DJ, Amnieh HB, Khandelwal M (2017) Development of a precise model for prediction of blast-induced flyrock using regression tree technique. Environ Earth Sci 76(1):27
5. Hasanipanah M, Shahnazar A, Amnieh HB, Armaghani DJ (2017) Prediction of air-overpressure caused by mine blasting using a new hybrid PSO–SVR model. Eng Comput 33(1):23–31
6. Hasanipanah M, Amnieh HB, Arab H, Zamzam MS (2016) Feasibility of PSO–ANFIS model to estimate rock fragmentation produced by mine blasting. Neural Comput Appl. https://doi.org/10.1007/s00521-016-2746-1
7. Dogan O, Anil Ö, Akbas SO, Kantar E, Tuğrul Erdem R (2013) Evaluation of blast-induced ground vibration effects in a new residential zone. Soil Dyn Earthq Eng 50:168–181
8. Faramarzi F, Ebrahimi Farsangi MA, Mansouri H (2014) Simultaneous investigation of blast induced ground vibration and airblast effects on safety level of structures and human in surface blasting. Int J Min Sci Technol 24:663–669
9. Richards AB, Moore AJ (2012) Blast vibration course: measurement, assessment, control. Terrock Consulting Engineers (Terrock Pty Ltd), Australia
10. Duvall WI, Petkof B (1959) Spherical propagation of explosion generated strain pulses in rock. USBM Rep Investig 548:21
11. Langefors U, Kilstrom B (1963) The modern technique of rock blasting. Wiley, New York
12. Davies B, Farmer IW, Attewell PB (1964) Ground vibration from shallow sub-surface blasts. Engineer 217:553–559
13. Ambraseys NR, Hendron AJ (1968) Dynamic behavior of rock masses: rock mechanics in engineering practices. In: Stagg K, Wiley J (eds) Rock mechanics in engineering practices. Wiley, London, pp 203–207
14. Bureau of Indian Standards (1973) Criteria for safety and design of structures subject to underground blasts, ISI Bulletin, IS-6922
15. Ghosh A, Daemen JK (1983) A simple new blast vibration predictor based on wave propagation laws. In: The 24th US symposium on rock mechanics (USRMS)
16. Gupta RN, Roy PP, Singh B (1987) On a blast induced blast vibration predictor for efficient blasting. In: Proceedings of the 22nd international conference on safety in Mines Research Institute, Beijing, China, pp 1015–1021
17. Roy PP (1991) Vibration control in an opencast mine based on improved blast vibration predictors. Min Sci Technol 12:157–165
18. Rai R, Singh TN (2004) A new predictor for ground vibration prediction and its comparison with other predictors. Indian J Eng Mater Sci 11:178–184
19. Khandewal M, Singh TN (2009) Prediction of blast-induced ground vibration using artificial neural network. Int J Rock Mech Min Sci 46:1214–1222
20. Ghasemi E, Ataei M, Hashemolhosseini H (2012) Development of a fuzzy model for predicting ground vibration caused by rock blasting in surface mining. J Vib Control 19:755–770
21. Hasanipanah M, Amnieh HB, Khamesi H, Armaghani DJ, Golzar SB, Shahnazar A (2016) Prediction of an environmental issue of mine blasting: an imperialistic competitive algorithm-based fuzzy system. Int J Environ Sci Technol. https://doi.org/10.1007/s13762-017-1395-y
22. Amiri M, Amnieh HB, Hasanipanah M, Khanli LM (2016) A new combination of artificial neural network and K-nearest neighbors models to predict blast-induced ground vibration and air-overpressure. Eng Comput 32:631–644
23. Fouladgar N, Hasanipanah M, Amnieh HB (2017) Application of cuckoo search algorithm to estimate peak particle velocity in mine blasting. Eng Comput 33(2):181–189
24. Dehghani H, Ataee-pour M (2011) Development of a model to predict peak particle velocity in a blasting operation. Int J Rock Mech Min Sci 48:51–58
25. Dindarloo SR (2015) Prediction of blast-induced ground vibrations via genetic programming. Int J Min Sci Technol 25:1011–1015
26. Iphar M, Yavuz M, Ak H (2008) Prediction of ground vibrations resulting from the blasting operations in an open-pit mine by adaptive neuro-fuzzy inference system. Environ Geol 56:97–107
27. Khandelwal M (2011) Blast-induced ground vibration prediction using support vector machines. Eng Comput 27:193–200
28. Fişne A, Kuzu C, Hüdaverdi T (2011) prediction of environmental impacts of quarry blasting operation using fuzzy logic. Environ Monit Assess 174:461–470
29. Monjezi M, Hasanipanah M, Khandelwal M (2013) Evaluation and prediction of blast-induced ground vibration at Shur River dam, Iran, by artificial neural network. Neural Comput Appl 22:1637–1643
30. Ghoraba S, Monjezi M, Talebi N, Jahed Armaghani D, Moghaddam MR (2016) Estimation of ground vibration produced by blasting operations through intelligent and empirical models. Environ Earth Sci 75:1137
31. Taheri K, Hasanipanah M, Golzar SB, Majid MZA (2016) A hybrid artificial bee colony algorithm-artificial neural network for forecasting the blast-produced ground vibration. Eng Comput 33(3):689–700
32. Hasanipanah M, Noorian–Bidgoli M, Armaghani DJ, Khamesi H (2016) Feasibility of PSO–ANN model for predicting surface settlement caused by tunnelling. Eng Comput 32(4):705–715
33. Mojtahedi S, Ebtehaj I, Hasanipanah M, Bonakdari H, Amnieh HB (2017) Proposing a novel hybrid intelligent model for the simulation of particle size distribution resulting from blasting. Eng Comput 33(2):307–316
34. Mokfi T, Shahnazar A, Bakhshayeshi I, Derakhsh AM, Tabrizi O (2018) Proposing of a new soft computing-based model to predict peak particle velocity induced by blasting. Eng Comput. https://doi.org/10.1007/s00366-018-0578-6
35. Hasanipanah M, Faradonbeh RS, Amnieh HB, Armaghani DJ, Monjezi M (2017) Forecasting blast-induced ground vibration developing a CART model. Eng Comput 33(2):307–316
36. Jiang W, Arslan CA, Tehrani MS, Khorami M, Hasanipanah M (2018) Simulating the peak particle velocity in rock blasting projects using a neuro-fuzzy inference system. Eng Comput. https://doi.org/10.1007/s00366-018-0659-6
37. Zadeh LZ (1993) Fuzzy logic, neural networks and soft computing". Microprocess Microprogramming 38:13
38. Khandelwal M, Singh TN (2006) Prediction of blast induced ground vibrations and frequency in opencast mine: a neural network approach. J Sound Vib 289:711–725
39. Khandewal M, Singh TN (2007) Evaluation of blast-induced ground vibration predictors. Soil Dyn Earthq Eng 27:116–125
40. Amnieh BH, Mozdianfard MR, Siamaki A (2010) Predicting of blasting vibrations in sarcheshmeh copper mine by neural network. Saf Sci 38:319–325
41. Monjezi M, Ahmadi M, Sheikhan M, Bahrami A, Salimi AR (2010) Predicting blast-induced ground vibration using various types of neural networks. Soil Dyn Earthq Eng 30:1233–1236
42. Monjezi M, Ghafurikalajahi M, Bahrami A (2011) Prediction of blast-induced ground vibration using artificial neural networks. Tunn Undergr Space Technol 26:46–50

43. Xue X, Yang X (2013) Predicting blast-induced ground vibration using general regression neural network. J Vib Control 20:1512–1519
44. Saadat M, Khandelwal M, Monjezi M (2014) An ANN-based approach to predict blast-induced ground vibration of Gol-E-Gohar Iron Ore Mine, Iran. J Rock Mech Geotech Eng 6:67–76
45. Álvarez-Vigil AE, González-Nicieza C, López Gayarre F, Álvarez-Fernández MI (2012) Predicting blasting propagation velocity and vibration frequency using artificial neural networks. Int J Rock Mech Min Sci 55:108–116
46. Görgülü K, Arpaz E, Demirci A, Koçaslan A, Dilmaç MK, Yüksek AG (2013) Investigation of blast-induced ground vibrations in the Tülü Boron Open Pit Mine. Bull Eng Geol Environ 72:555–564
47. Lapčević R, Kostić S, Pantović R, Vasović N (2014) Prediction of blast-induced ground motion in a copper mine. Int J Rock Mech Min Sci 69:19–25
48. Görgülü K, Arpaz E, Uysa Ö, Durutürk AG, Yüksek AG, Koçaslan A, Dilmaç MK (2015) Investigation of the effects of blasting design parameters and rock properties on blast-induced ground vibrations. Arab J Geosci 8:4269–4278
49. Shahri AA, Asheghi A (2018) Optimized developed artificial neural network-based models to predict the blast-induced ground vibration. Innov Infrastruct Solut 3:34
50. Iramina WS, Sansone EC, Wichers M, Wahyudi S, Eston SM, Shimada H, Sasaoka T (2018) Comparing blast-induced ground vibration models using ANN and empirical geomechanical relationships. REM Int Eng J 71:89–95
51. Huang GB, Zhu QY, Siew CK (2006) Extreme learning machine: theory and applications. Neurocomputing 70:489–501
52. Huang Y (2009) Advances in artificial neural networks—methodological development and application. Algorithms 2:973–1007
53. Adeel A, Larijani H, Javed A, Ahmadinia A (2015) Impact of learning algorithms on random neural network based optimization for LTE-UL systems. Netw Protoc Algorithms 7:157–178
54. Samui P (2014) Utilization of Gaussian process regression for determination of soil electrical resistivity. Geotech Geol Eng 32:191–195
55. Liu J, Yan K, Zhao X, Hu Y (2016) Prediction of autogenous shrinkage of concretes by support vector machine. Int J Pavement Res Technol 9:169–177
56. Ažman K, Kocijan J (2007) Application of Gaussian processes for black-box modelling of biosystems. ISA Trans 46:443–457
57. Samui P, Jagan J (2013) Determination of effective stress parameter of unsaturated soils: a Gaussian process regression approach. Front Struct Civ Eng 7:133–136
58. Bin S, Wenlai Y (2013) Application of Gaussian process regression to prediction of thermal comfort index. In: 11th IEEE international conference on electronic measurement & instruments, Harbin, China, pp 958–961
59. Dong D (2012) Mine gas emission prediction based on Gaussian process model. Procedia Eng 45:334–338
60. Kong D, Chen Y, Li N (2018) Gaussian process regression for tool wear prediction. Mech Syst Signal Process 104:556–574
61. Gao W, Karbasi M, Hasanipanah M, Zhang X, Guo J (2018) Developing GPR model for forecasting the rock fragmentation in surface mines. Eng Comput 34:339–345
62. Appianing EJA (2013) A review of waste dump reclamation practices at GMC Nsuta. Dissertation, University of Mines and Technology, Tarkwa
63. Apalangya PA (2014) An assessment of the blast practices at Pit C of Ghana Manganese Company Limited. Dissertation, University of Mines and Technology, Tarkwa
64. Hagan MT, Demuth HB, Beale MH, De Jesús O (1996) Neural network design. Pws Pub, Boston
65. Yegnanarayana B (2005) Artificial neural networks. Prentice-Hall of India Private Limited, New Delhi
66. Ghosh J, Nag A (2001) An overview of radial basis function networks. In: Howlett RJ, Jain LC (eds) Radial basis function network 2, 1st edn. Springer, Berlin, pp 1–36
67. Specht DF (1991) A General regression neural network. IEEE Trans Neural Netw 2(6):568–576
68. Rasmussen CE, Williams CKI (2006) Gaussian processes for machine learning. The MIT Press, Cambridge
69. Li JJ, Jutzeler A, Faltings B (2014) Estimating urban ultrafine particle distributions with Gaussian process models. In: Winter S, Rizos C (eds) Proceedings of Research@Locate'14, Canberra, Australia, 7th–9th April, 2014, pp 145–153
70. Kang F, Han S, Salgado R, Li J (2015) System probabilistic stability analysis of soil slopes using Gaussian process regression with Latin Hypercube sampling. Comput Geotech 63:13–25
71. Snelson EL (2007) Flexible and efficient Gaussian process models for machine learning. Dissertation, University of London
72. Moore CJ, Chua AJK, Berry CPL, Gair JR (2016) Fast methods for training Gaussian process on large datasets. R Soc Open Sci 3:1–10
73. Mueller AV, Hemond HF (2013) Extended artificial neural networks: incorporation of a priori chemical knowledge enables use of ion selective electrodes for in-situ measurement of ions at environmentally relevant levels. Talanta 117:112–118
74. Savaux V, Bader F (2015) Mean square error analysis and linear minimum mean square error application for preamble-based channel estimation in orthogonal frequency division multiplexing/offset quadrature amplitude modulation systems. IET Commun 9(14):1763–1773
75. Chai T, Draxler RR (2014) Root mean square error (RMSE) or mean absolute error (MAE)? Arguments against avoiding RMSE in the literature. Geosci Model Dev 7:1247–1250
76. Asuero AG, Sayago A, González AG (2006) The correlation coefficient: an overview. Crit Rev Anal Chem 36:41–59
77. Hasanipanah M, Armaghani DJ, Khamesi H, Amnieh HB, Ghoraba S (2016) Several non-linear models in estimating air-overpressure resulting from mine blasting. Eng Comput 32(3):441–455
78. Hasanipanah M, Naderi R, Kashir J, Noorani SA, Qaleh AZA (2017) Prediction of blast-produced ground vibration using particle swarm optimization. Eng Comput 33(2):173–179
79. Hasanipanah M, Armaghani DJ, Amnieh HB, Majid MZA, Tahir MMD (2017) Application of PSO to develop a powerful equation for prediction of flyrock due to blasting. Neural Comput Appl 28:1043–1050. https://doi.org/10.1007/s00521-016-2434-1
80. Hornik K, Stinchcombe M, White H (1989) Multilayer feed forward networks are universal approximators. Neural Netw 2:359–366
81. Moré JJ (1978) The Levenberg–Marquardt algorithm: implementation and theory. In: Watson GA (ed) Numerical analysis, vol 630. Lecture notes in mathematics. Springer, Berlin, Heidelberg, pp 105–116
82. Ruder S (2016) An overview of gradient descent optimisation algorithms. arXiv preprint http://arxiv.org/abs/1609.04747
83. Mohammadnejad M, Gholami R, Ramezanzadeh A, Jalali ME (2011) Prediction of blast-induced vibrations in limestone quarries using support vector machine. J Vib Control 18(9):1322–1329
84. Ragam P, Nimaje DS (2018) Assessment of blast-induced ground vibration using different predictor approaches—a comparison. Chem Eng Trans 66:487–492
85. Armaghani DJ, Hajihassani M, Mohamad ET, Marto A, Noorani SA (2014) Blasting-induced flyrock and ground vibration prediction through an expert artificial neural network based on particle swarm optimization. Arab J Geosci 7(12):5383–5396

86. Tiile RN (2016) Artificial neural network approach to predict blastinduced ground vibration, airblast and rock fragmentation. Dissertation, Missouri University of Science and Technology
87. Delis I, Panzeri S, Pozzo T, Berret B (2013) A unifying model of concurrent spatial and temporal modularity in muscle activity. J Neurophysiol 111:675–693